Comparison of regulated passive membrane conductance in action potential–firing fast- and slow-twitch muscle

Thomas Holm Pedersen,[1] William Alexander Macdonald,[1] Frank Vincenzo de Paoli,[1] Iman Singh Gurung,[2] and Ole Bækgaard Nielsen[1]

[1]Department of Physiology and Biophysics, University of Aarhus, DK-8000 Århus C, Denmark
[2]Physiological Laboratory, University of Cambridge, Cambridge CB2 1TN, England UK

In several pathological and experimental conditions, the passive membrane conductance of muscle fibers (G_m) and their excitability are inversely related. Despite this capacity of G_m to determine muscle excitability, its regulation in active muscle fibers is largely unexplored. In this issue, our previous study (Pedersen et al. 2009. *J. Gen. Physiol.* doi:10.1085/jgp.200910291) established a technique with which biphasic regulation of G_m in action potential (AP)-firing fast-twitch fibers of rat extensor digitorum longus muscles was identified and characterized with temporal resolution of seconds. This showed that AP firing initially reduced G_m via ClC-1 channel inhibition but after ∼1,800 APs, G_m rose substantially, causing AP excitation failure. This late increase of G_m reflected activation of ClC-1 and K_{ATP} channels. The present study has explored regulation of G_m in AP-firing slow-twitch fibers of soleus muscle and compared it to G_m dynamics in fast-twitch fibers. It further explored aspects of the cellular signaling that conveyed regulation of G_m in AP-firing fibers. Thus, in both fiber types, AP firing first triggered protein kinase C (PKC)-dependent ClC-1 channel inhibition that reduced G_m by ∼50%. Experiments with dantrolene showed that AP-triggered SR Ca^{2+} release activated this PKC-mediated ClC-1 channel inhibition that was associated with reduced rheobase current and improved function of depolarized muscles, indicating that the reduced G_m enhanced muscle fiber excitability. In fast-twitch fibers, the late rise in G_m was accelerated by glucose-free conditions, whereas it was postponed when intermittent resting periods were introduced during AP firing. Remarkably, elevation of G_m was never encountered in AP-firing slow-twitch fibers, even after 15,000 APs. These observations implicate metabolic depression in the elevation of G_m in AP-firing fast-twitch fibers. It is concluded that regulation of G_m is a general phenomenon in AP-firing muscle, and that differences in G_m regulation may contribute to the different phenotypes of fast- and slow-twitch muscle.

INTRODUCTION

In our companion paper (see Pedersen et al. in this issue), we presented a new technique that allows determination of G_m in action potential (AP)-firing muscle fibers with a temporal resolution of seconds. Using this approach, we identified biphasic regulation of G_m in AP-firing fast-twitch extensor digitorum longus (EDL) muscle fibers. In the first phase, Phase 1, the onset of AP firing led to a reduction in G_m that was caused by reduced resting membrane conductance for Cl^- (G_{Cl}) via underlying inhibition of ClC-1 channels. The second phase, Phase 2, was initiated after prolonged AP firing and was characterized by a dramatic rise in G_m that reflected greatly elevated resting membrane conductance for K^+ (G_K) in combination with elevated G_{Cl}. We further showed that the ion channels underlying the elevated G_K and G_{Cl} during Phase 2 were K_{ATP} and ClC-1 channels, respectively. Intriguingly, the elevations in G_K and G_{Cl} occurred synchronously during Phase 2, indicating that the K_{ATP} and ClC-1 channels responded to similar cellular signaling.

In this study, we further explore G_m dynamics in AP-firing muscle fibers by comparing G_m between fast- and slow-twitch muscle fibers. This comparative approach proved useful for two reasons. First, it allowed us to assess whether regulation of G_m is a general phenomenon in skeletal muscle or only restricted to fast-twitch muscle. Thus, it was possible to evaluate whether differences in G_m dynamics in active muscle fibers could contribute to phenotypic differences between fast- and slow-twitch muscle fibers. Second, because G_m dynamics in fast-twitch muscle fibers predominantly reflected underlying regulation of ClC-1 and K_{ATP} channels and these channels are expressed in both fiber types, the comparative approach could reveal how ion channel regulation depends on the cellular environment. In particular, because slow-twitch fibers have much larger oxidative capacity than fast-twitch fibers (Jackman and Willis, 1996;

Correspondence to Thomas Holm Pedersen: thp@fi.au.dk

Abbreviations used in this paper: AP, action potential; BTS, *N*-benzyl-*p*-toluene sulphonamide; EDL, extensor digitorum longus; Pbdu, phorbol 12,13-dibutyrate; pH_i, intracellular pH.

The Rockefeller University Press $30.00
J. Gen. Physiol. Vol. 134 No. 4 323–337
www.jgp.org/cgi/doi/10.1085/jgp.200910291

Mogensen and Sahlin, 2005), the comparative approach allowed the same ion channels to be studied under different settings of cellular maintenance of metabolic status during repeated AP firing.

MATERIALS AND METHODS

Animal handling and muscle preparation

The aim of this study was to explore G_m dynamics during muscle activity in fast- and slow-twitch muscle fibers. Consequently, experiments were performed using either rat EDL muscle to represent typical fast-twitch fibers or rat soleus muscles that almost exclusively contain type I slow-twitch fibers (Edström et al., 1982). Experiments for G_m determinations used muscle from 12–14-wk-old female Wistar rats (~230 g), whereas for contraction experiments, muscles from male or female 4–5-wk-old animals (~70 g) were used. The handling and killing of animals followed Danish animal welfare regulations. The standard Krebs-Ringer bicarbonate solution and the solutions containing reduced or no Cl^- were prepared as described in our companion paper (Pedersen et al., 2009). Solutions with 10 rather than 4 mM K^+ were made by substitution of KCl for NaCl. All experiments were conducted at 30°C. GF109203X, Gö6993, *N*-benzyl-*p*-toluene sulphonamide (BTS), dantrolene, phorbol 12,13-dibutyrate (Pbdu), and blebbistatin were dissolved in DMSO. The maximal concentration of DMSO in experimental solutions was 0.15%, which did not affect resting conditions in muscles.

Determination of the passive membrane conductance in AP-firing fibers

To determine G_m in AP-firing fibers, the technique and methods of calculating G_{Cl} and G_K developed in our previous study (Pedersen et al., 2009) were used. In brief, direct measurements of the input conductance in between successive AP trains were used to extract G_m in AP-firing fibers. This required that the passive membrane conductance was assessed before AP firing (G_{mS}) in a subset of muscle fibers under the appropriate experimental conditions. Values of G_ms under the various experimental conditions are shown in Table I. The protocol for current injections, data sampling, filter settings, electrode resistance, and electrode solutions (2 M K-citrate) were all identical to those in our previous study.

Blebbistatin was used to block contractile activity in soleus muscles

To measure the input conductance in between successive AP trains without encountering problems of microelectrode breakage due to contractile activity, the myosin II of the contractile proteins was inhibited using specific inhibitors. In most experiments with fast-twitch fibers, myosin II was inhibited using 50 µM BTS, which only reduces the energy consummation of active EDL muscles by ~20% (Zhang et al., 2006). However, because BTS is specific for myosin II of fast-twitch fibers (Cheung et al., 2002; Macdonald et al., 2005), an alternate myosin II inhibitor, blebbistatin (25 µM) (Straight et al., 2003; Limouze et al., 2004), which inhibits contractions in both fast- and slow-twitch fibers (Fig. S1), was used in experiments with soleus muscles. To evaluate whether blebbistatin was an appropriate experimental tool for the present study, it was important to ensure that it did not markedly affect the excitability of the muscle fibers. Thus, a series of experiments was conducted to investigate for effects of blebbistatin on the excitability and force in both EDL and soleus muscles. In brief, these control experiments showed that blebbistatin was able to block the contractile force in whole EDL and soleus muscle (Fig. S1). It did not interfere with the resting membrane potential or G_{mS} (Table S1). There was no change in the ionic contents of Na^+ or K^+ with the drug and it did not interfere with the Na^+/K^+-pump activity (Table S1). Blebbistain did not affect the AP peaks, nor did it in any dramatic way affect the shape of the APs (Table S1). The only consistent effect of blebbistatin was an increase in the rheobase current; i.e., the current required to be injected to elicit an AP (Table S1). To further evaluate blebbistatin as an experimental tool, a series of experiments was conducted to compare G_m dynamics in AP-firing EDL fibers that had been treated with blebbistatin with G_m dynamics in BTS-treated fibers (Fig. 1). In experiments with blebbistatin-treated fibers, a biphasic development of G_m was observed that appeared indistinguishable from observations in BTS-treated fibers. Collectively, these experiments showed that blebbistatin could be used as an experimental tool to block contractile activity during AP firing in both fast- and slow-twitch muscle fibers.

Intracellular pH (pH_i) measurements

Measurements of pH_i were performed using an epifluorescence system as described previously (de Paoli et al., 2007). In brief, BTS-treated EDL muscles were loaded with 20 µM 2′,7′-bis(2-carboxyethyl)-5(6)-carboxyfluorescein (BCECF-AM) for ~30 min and then washed. Whole muscles were stimulated to fire APs using field stimulation with protocols similar to those used in the single-electrode experiments. The emission ratio of BCECF-loaded muscle was calibrated to pH_i by the K^+-nigericin technique (Thomas et al., 1979).

Contractions in whole muscle

Force production and M-waves were assessed in intact EDL and soleus muscles using an experimental setup that has been extensively described previously (Nielsen et al., 2001; Macdonald et al., 2005; Pedersen et al., 2005). Tetanic contractions were elicited via field stimulation at 30 V/cm for 2 (soleus) or 0.5 s (EDL) using 60-Hz trains of 0.02-ms pulses every 10 (soleus) or 20 min (EDL).

Quantification of G_m dynamics and statistics

In our companion paper (Pedersen et al., 2009), the biphasic dynamics of G_m in AP-firing fast-twitch fibers was well described by Eqs. 1 and 2. This approach for quantification was also used in the present study.

$$G_{m.Phase1} = G_{mS} + A_1(1-\exp(-t/\tau_1)) \quad (1)$$

$$G_{m,Phase2} = G_{mS} + A_1 + \frac{A_2}{1+\exp(\frac{\tau_2 - t}{\beta})} \quad (2)$$

Thus, Phase 1 was described by a single-exponential function containing information on the amplitude of the reduction in G_m during Phase 1, A_1, and how fast this reduction occurred, τ_1. Phase 2 was described by a sigmoidal function that quantified the magnitude of the rise in G_m during Phase 2, A_2, when G_m rose, τ_2, and how fast G_m rose, β, during Phase 2. The dynamics of G_m in soleus fibers was reminiscent of Phase 1 in EDL fibers, and it was well quantified by Eq. 1. Statistical analysis of data was performed as described in Pedersen et al. (2009).

Chemicals and isotope

All chemicals were of analytical grade. BTS and blebbistatin were from Toronto Research Chemicals Inc., and GF109203X (bisindolylmaleimide I), Gö6976, Pbdu, and dantrolene were from Sigma-Aldrich. BCECF-AM was from Invitrogen. $^{86}Rb^+$ (1,590 GBq $mmol^{-1}$) was from PerkinElmer.

TABLE I

G_{mS} in Soleus and EDL muscle fibres before AP firing ($\mu S/cm^2$)

Muscle fiber type	Group	Treatment	G_{mS}	$G_{mS,50}$	G_{KS}	$G_{ClS,127}$	$G_{ClS,50}$
			($\mu S/cm^2$)	*($\mu S/cm^2$)*	*($\mu S/cm^2$)*	*($\mu S/cm^2$)*	*($\mu S/cm^2$)*
EDL[a]	50 µM BTS	—	1,458 ± 70 (n = 26/7)	361 ± 21 (n = 15/4)	144 ± 16 (n = 13/6)	1,314 ± 72	217 ± 26
EDL	25 µM blebbistatin	—	1,317 ± 71 (n = 12/4)	—	—	—	—
EDL	50 µM BTS	25 µM dantrolene	1,538 ± 80 (n = 32/5)	—	—	—	—
EDL	50 µM BTS	1 µM GF109203X	1,527 ± 115 (n = 12/2)	—	—	—	—
EDL	50 µM BTS	Glucose free	1,622 ± 126 (n = 11/2)	—	—	—	—
Soleus	25 µM blebbistatin	—	970 ± 61 (n = 42/8)	289 ± 29 (n = 18/4)	191 ± 13 (n = 25/4)	779 ± 62	98 ± 26
Soleus	25 µM blebbistatin	1 µM GF109203X	1,306 ± 92 (n = 28/5)	—	—	—	—

Subscript "S" indicates values for G_m before AP firing under the various experimental conditions as determined using the classical technique (Pedersen et al., 2009). $G_{mS,50}$ represents G_m before AP firing at 50 mM Cl^-. G_{KS} and G_{ClS} represent component conductances of G_{mS} for K^+ and Cl^-, respectively, whereas $G_{ClS,50}$ represents the component conductance of $G_{mS,50}$ for Cl^-. All data are presented as means ± SEM.
[a]Included from our companion paper (Pedersen et al., 2009).

Online supplemental material

The online supplemental material contains the outcome from experiments where the effects of blebbistatin on the excitability of EDL and soleus muscles were evaluated. It is available at http://www.jgp.org/cgi/content/full/jgp.200910291/DC1.

RESULTS

Comparison of G_m dynamics in AP-firing fast- and slow-twitch fibers

In the initial series of experiments, G_m dynamics were determined in AP-firing muscle fibers from fast-twitch EDL or slow-twitch soleus muscles. Fig. 1 (B and C) shows representative recordings of the membrane potential from an EDL fiber (Fig. 1 B) and from a soleus fiber (Fig. 1 C) during experiments in which the fibers were activated to fire 3.5-s AP trains at 15 Hz repeatedly every 7 s. In the EDL fiber, the onset of AP firing was associated with an increased ΔV, and when AP firing was continued beyond ∼1,800 APs, ΔV suddenly dropped to less than half of its value before AP firing. These observations in the EDL fiber reflect the biphasic dynamics of G_m in AP-firing EDL fibers that we presented in the companion paper (Pedersen et al., 2009). In the soleus fiber, the onset of AP firing was similarly associated with increased ΔV but, in marked contrast to the observations in the EDL fiber, the drop in ΔV never appeared, even after >15,000 APs. Such experimental observations of ΔV in AP-firing fibers were next converted to G_m using Eq. 3 from Pedersen et al. (2009). Fig. 1 D shows the average G_m from EDL fibers that were stimulated to fire AP trains of either 15 or 30 Hz, and Fig. 1 E shows the dynamics of G_m in AP-firing soleus fibers that were stimulated to fire AP trains of 6, 15, 30, or 60 Hz. Fig. 1 (D and E) shows that the onset of AP firing was associated with substantial reductions in G_m in both muscle fiber types and at all frequencies. When comparing these initial reductions of G_m between fast- and slow-twitch fibers, the reductions appeared to be of similar magnitudes, but they developed substantially faster in EDL fibers than in soleus fibers. Indeed, when the reduction in G_m at the onset of AP firing was fitted to Eq. 1, the magnitudes of the G_m reductions, A_1, reached 45–70% and 43–55% of G_m at the start of the experiments in soleus and EDL fibers, respectively, whereas the time required for the development of the reductions, τ_1, was substantially longer in the slow-twitch fibers (60 ± 9 and 76 ± 9 s at 15 and 30 Hz, respectively; Table II) than in the fast-twitch fibers (32 ± 4 and 17 ± 1 s at 15 and 30 Hz, respectively; Table II). However, the most striking difference between fast- and slow-twitch muscle fibers was the complete absence of a rise in G_m with prolonged AP firing in slow-twitch fibers. Thus, comparing Fig. 1 (D and E) also shows that in clear contrast to the massive rise in G_m after prolonged AP firing in EDL fibers (Phase 2), G_m remained low throughout all experiments and at all frequencies in the soleus fibers, even if the AP firing was continued for much longer.

Note also that the observations in the EDL fibers presented in Fig. 1 D were obtained using blebbistatin as a myosin II inhibitor. These very closely replicated the observations in our previous study, where BTS rather than blebbistatin was used to inhibit contractile activity during AP firing. Thus, none of the parameters used to quantify Phase 1 (A_1 and τ_1) and Phase 2 (A_2, τ_2, and β)

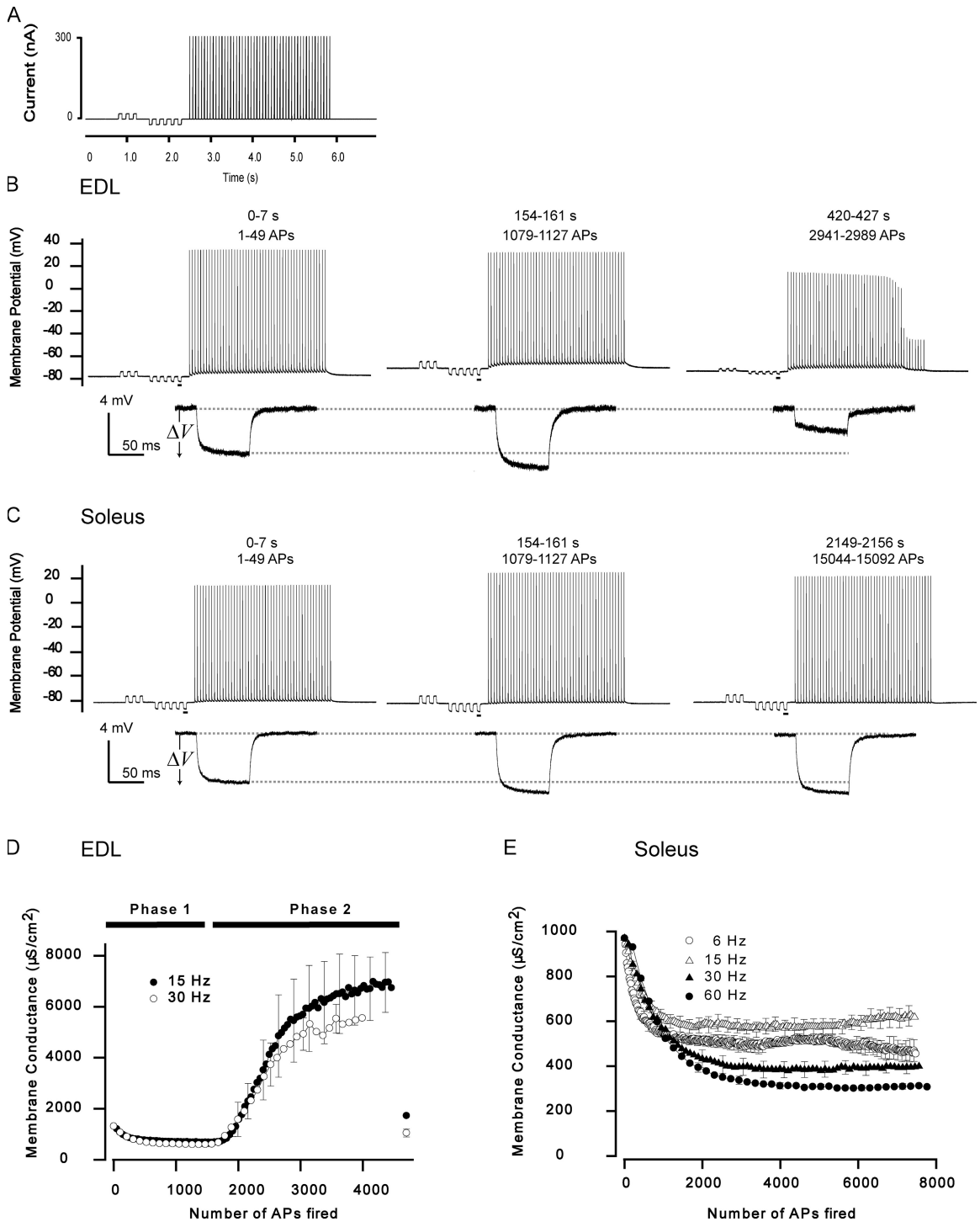

Figure 1. The onset of AP firing was associated with reduced G_m in both fast- and slow-twitch fibers, whereas prolonged AP firing induced a massive elevation in G_m only in fast-twitch fibers. For experiments, electrodes were inserted into a fiber at close proximity (~70 μm). One electrode repeatedly injected a current protocol while the other electrode recorded the membrane potential. (A) Current injection protocol that consisted of low amplitude (±10–20 nA) pulses, which were used for G_m determination, and the train of AP trigger pulses (3 ms and 300 nA) that could be delivered at variable frequency, here as 15 Hz. This protocol was repeated without intermittent breaks until the fiber had been exposed to ~5,000 trigger AP pulses in EDL or up to 15,000 pulses in soleus fibers. (B) Representative recordings of AP trains in a fast-twitch EDL fiber during the first, the 23rd, and the 61st AP train. Note the dropout of APs at the end of the AP train on the right. (C) Representative recordings of AP trains in a slow-twitch soleus fiber during the first, the 23rd, and the 308th AP train. In B and C, the experimental durations and the total number of AP trigger pulses are shown above the AP trains. G_m was calculated from the voltage deflections, ΔV, resulting from the small current pulses between the successive AP trains. The underlined ΔVs have been enlarged below the representative traces. (D) The biphasic dynamics of G_m in AP-firing EDL fibers treated with blebbistatin

were different between EDL fibers treated with the two types of myosin II inhibitors (Table II).

Ion channels involved in G_m dynamics in AP-firing slow-twitch fibers

To explore which ion channels that were involved in the reduction in G_m in AP-firing soleus fibers, G_K and G_{Cl} were determined using the approach described in our previous study (Pedersen et al., 2009). This required experimental observation of G_m dynamics at two extracellular Cl^- concentrations (Eq. 4 in Pedersen et al., 2009). Thus, Fig. 2 A shows the dynamics of G_m at 50 and 127 mM Cl^- with an AP-firing frequency of 30 Hz. Two major effects of reduced Cl^- were apparent. First, the resting membrane conductance before AP firing was reduced substantially (Table I). Second, AP firing was associated with an initial increase in G_m, followed by a slight reduction in G_m, whereas at 127 mM Cl^-, G_m became reduced from the onset of AP firing. This indicated that the reduction of G_m in AP-firing soleus fibers could largely be ascribed to reduced G_{Cl}. This notion was confirmed by calculations of G_K and G_{Cl} (Fig. 2 B), which demonstrated that the reduced G_m in AP-firing soleus fibers reflected the net outcome of a pronounced reduction in G_{Cl} and a slight increase in G_K. Similar changes in G_K and G_{Cl} were observed in soleus fibers stimulated with AP trains of 6 and 60 Hz (not depicted). Because ClC-1 channels are the major Cl^- channel in muscle (Koch et al., 1992; Lueck et al., 2007) this shows that, similar to the situation in EDL fibers (Pedersen et al., 2009), the onset of AP firing in soleus fibers leads to ClC-1 channel inhibition and a minor activation of K^+ channels.

Cellular mechanism underlying ClC-1 inhibition at the onset of AP firing

The above experiments showed that inhibition of ClC-1 channels at the onset of AP firing was common to both fiber types. It has previously been demonstrated experimentally that the resting membrane conductance for Cl^- can be reduced in muscle fibers either by acidosis (Hutter and Warner, 1967; Pedersen et al., 2004, 2005) or by activation of PKC (Tricarico et al., 1991; Rosenbohm et al., 1999; Pierno et al., 2007; Dutka et al., 2008).

First, to explore for a role of PKC in the ClC-1 channel inhibition at the onset of AP firing, experiments were conducted in which the muscles were pretreated with a PKC inhibitor, GF109203X (Toullec et al., 1991). Under such conditions, the reduction in G_m at the onset of AP firing was largely abolished in both fiber types. Thus, Fig. 3 A shows observations from an EDL muscle

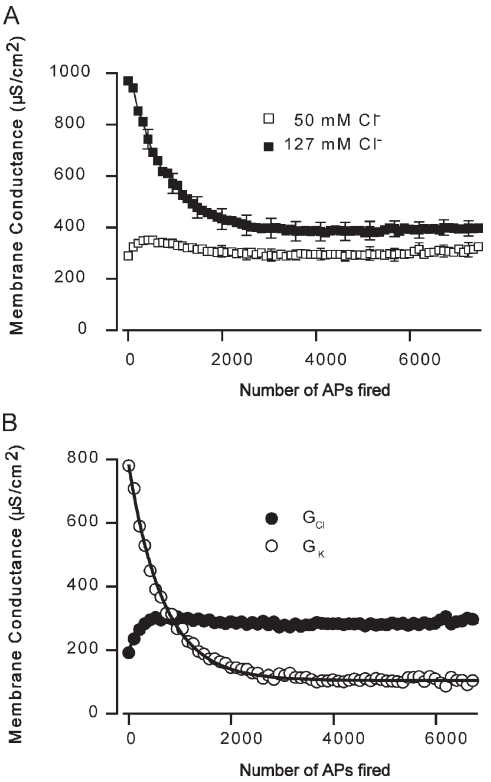

Figure 2. Component conductances, G_K and G_{Cl}, in slow-twitch soleus fibers firing APs. From experiments conducted at two concentrations of extracellular Cl^-, it was possible to extract G_K and G_{Cl} using Eq. 4 from Pedersen et al. (2009). (A) G_m dynamics at 50 and 127 mM Cl^- obtained using AP trains of 30 Hz. (B) Calculated G_K and G_{Cl}. Average data are presented as mean ± SEM.

fiber pretreated with the inhibitor during the first, the 22nd, and the 70th AP train. The enlarged recordings of ΔV below the AP trains show that the increase in ΔV that was usually observed at the onset of AP firing was completely abolished by the inhibitor, whereas the drop in ΔV during prolonged AP firing was still present with PKC inhibition. Fig. 3 B shows that the increase in ΔV at the onset of AP firing could also be abolished by the PKC inhibitor in a soleus fiber. Fig. 3 (C and D) presents the average G_m with the inhibitor in 11 EDL fibers (Fig. 3 C) and in 5 soleus fibers (Fig. 3 D). In the soleus fibers, the PKC inhibitor completely abolished the reduction in G_m at the onset of AP firing, whereas in the EDL fibers, a minor reduction of G_m that reached 81 ± 4% of the G_m at the start of the experiments in EDL could still be detected with the inhibitor. This reduction in EDL fibers was, however, much less than the reduction of G_m in control fibers, where it became reduced to 45 ± 4% of its value at the start of the experiment. Furthermore, the reduction in G_m in the EDL fibers with the PKC inhibitor appeared to occur later than the reduction

to inhibit myosin II. Fibers were stimulated with AP trains of either 15 or 30 Hz. (E) The G_m dynamics in AP-firing soleus fibers. Fibers were stimulated with AP trains of 6, 15, 30, or 60 Hz. Average data are presented as mean ± SEM.

TABLE II

Parameters obtained by fitting blebbistatin observations of G_m at 15 or 30 Hz to Eqs. 5 and 6

Muscle fiber type	Group	Myosin II inhibitor	A_1	τ_1	τ_1 (APs)	A_2	τ_2	τ_2 (APs)	β	β (APs)
			(μS/cm²)	*(s)*		*(μS/cm²)*	*(s)*		*(s)*	
EDL	15 Hz (n = 5)	Blebbistatin	−624 ± 67	32 ± 4	225 ± 30	6,144 ± 1,239	383 ± 35	2,680 ± 248	31 ± 3	219 ± 19
EDL	30 Hz (n = 6)	Blebbistatin	−718 ± 51	17 ± 1	256 ± 18	4,697 ± 523	161 ± 8	2,417 ± 127	13 ± 1	193 ± 8
EDL[a]	6 Hz (n = 8)	BTS	−779 ± 78	66 ± 8	199 ± 24	3,400 ± 431	1,088 ± 79	3,264 ± 237	79 ± 14	238 ± 43
EDL[a]	15 Hz (n = 18)	BTS	−809 ± 39	27 ± 1	189 ± 10	5,426 ± 494	352 ± 12	2,466 ± 81	34 ± 2	237 ± 12
EDL[a]	30 Hz (n = 13)	BTS	−706 ± 50	18 ± 1	273 ± 14	4,157 ± 575	174 ± 9	2,611 ± 129	26 ± 2	383 ± 37
Soleus	6 Hz (n = 5)	Blebbistatin	−441 ± 34	109 ± 25	327 ± 73	—	—	—	—	—
Soleus	15 Hz (n = 9)	Blebbistatin	−415 ± 28	76 ± 9	494 ± 60	—	—	—	—	—
Soleus	30 Hz (n = 7)	Blebbistatin	−588 ± 30	60 ± 9	897 ± 137	—	—	—	—	—
Soleus	60 Hz (n = 8)	Blebbistatin	−672 ± 12	35 ± 3	1,069 ± 93	—	—	—	—	—

Experimental observations of G_m in AP-firing fibers were fitted to Eqs. 1 and 2 to obtain parameters that describe Phase 1 and Phase 2 in EDL and the reduction of G_m at the onset of AP firing in soleus. A_1 represents the reduction in G_m at the onset of AP firing, whereas τ_1 describes either the time required or the number of APs fired before 63% of A_1 was observed. A_2 represents the magnitude of the increase in G_m during Phase 2, and τ_2 stands for the time or the number of APs that was fired before G_m had risen to half of A_2. β reflects the steepness of the rise of G_m during Phase 2. All data are presented as means ± SEM.

[a]Included from our companion paper (Pedersen et al., 2009).

in control fibers and, accordingly, G_m in the fibers treated with the PKC inhibitor could not be quantified by fitting to Eq. 1. In contrast, to the effect of PKC inhibition on the reduction of G_m at the onset of AP firing, the PKC-inhibited EDL fibers developed a pronounced increase in G_m with prolonged AP firing that was very similar to the increased G_m during Phase 2 in control fibers. In an additional series of experiments with four EDL fibers, which had been pretreated with an alternate PKC inhibitor, Gö6976, G_m was only reduced to 79 ± 11% of the G_m at the start of the experiment during Phase 1, whereas a pronounced increase of G_m was also observed during Phase 2 in these fibers.

In our previous study (Pedersen et al., 2009), the ClC-1 channel inhibition during Phase 1 in EDL fibers was demonstrated to be independent of whether the APs were triggered using inserted electrodes or whether the APs were triggered via the more physiological approach of motor nerve stimulation. To ensure that PKC activation was also activated during such motor nerve stimulation, whole muscles were stimulated to fire 686 APs, after which the two electrodes were rapidly inserted (<1 min) to monitor the recovery of G_{in} after AP firing. Although muscle contractions were clearly visible during the motor nerve stimulation, Fig. 5 E shows that after the AP firing, G_{in} was still high and did not display any change throughout 7 min of recovery in the fibers treated with the PKC inhibitor. This contrasted the rise in G_{in} that was observed after identical motor nerve stimulation in muscles without the inhibitor (Fig. 3 E).

Second, despite the very clear involvement of PKC in the fast reduction of G_m at the onset of AP firing (Fig. 3), it was possible that acidosis played a role for activating PKC or was involved in the delayed reduction of G_m during Phase 1 in the EDL fibers treated with the PKC inhibitor. Thus, to evaluate the role of acidosis for the reduction in G_m at the onset of AP firing, recordings of pH_i in whole, field-stimulated BTS-treated EDL muscle was compared with the observed G_m dynamics during Phase 1. Fig. 4 A shows that the development of pH_i had similar magnitudes when muscles were stimulated using AP trains of 6, 15, or 30 Hz. Also, the changes in pH_i appeared to depend on the number of APs fired rather than on the duration of the experiment (Fig. 4 A). Hence, during the first 500 APs, pH_i either rose a little or remained constant, and then it began to drop. The lowest pH_i occurred after ∼1,500 APs. In Fig. 4 (B–D), the dynamics of pH_i and G_m have been plotted against time for observations at 6 (Fig. 4 B), 15 (Fig. 4 C), and 30 Hz (Fig. 4 D). Comparing the dynamics of pH_i and G_m shows that although pH_i did not change markedly during the first 500 APs, this was actually the period when the largest decline in G_m occurred. This strongly indicated that the PKC-mediated ClC-1 channel inhibition at the onset of AP firing was not triggered by acidification. However, in the EDL fibers exposed to PKC inhibition,

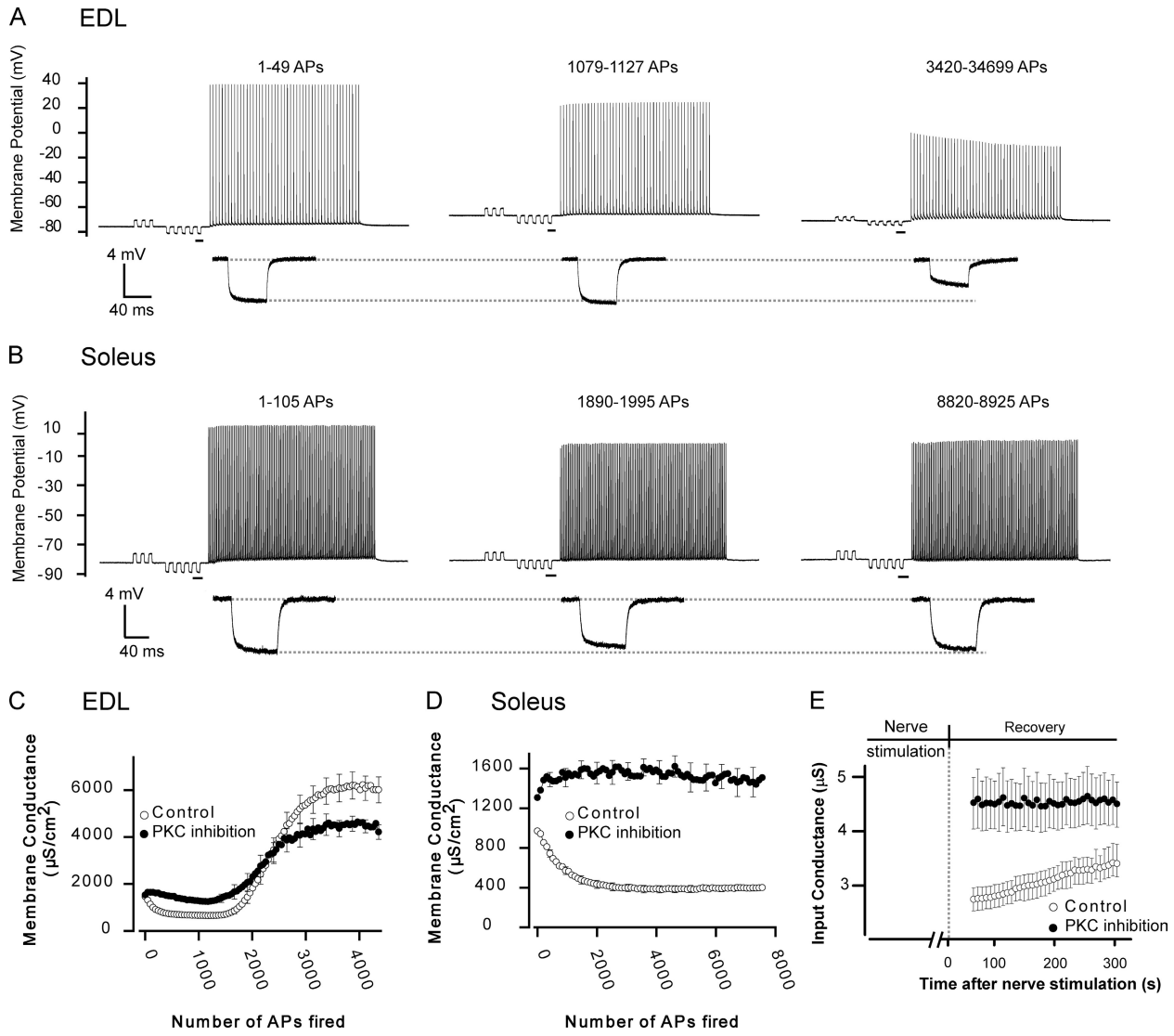

Figure 3. PKC inhibition removes the reduction in G_m at the onset of AP firing. Muscles were exposed to 1 μM of the PKC inhibitor GF109203X and stimulated by injecting the current protocol shown in Fig. 1 A with either 15- or 30-Hz trains. (A) Representative recordings of 15-Hz AP trains in an EDL fiber exposed to the PKC inhibitor. (B) Representative recordings of 30-Hz AP trains in a soleus fiber exposed to the PKC inhibitor. The underlined ΔV has been enlarged below the representative traces. (C) The average G_m in 11 AP-firing EDL fibers exposed to the PKC inhibitor. (D) The average G_m in five AP-firing soleus fibers exposed to the PKC inhibitor. In C and D, G_m at control conditions has been included for comparison. (E) The effect of PKC inhibition on the recovery of G_{in} in EDL fibers after whole muscle stimulation via the motor nerve. Average data are presented as mean ± SEM.

a minor reduction in G_m during the early stages of AP firing was still observed (Fig. 3 C). When the dynamics in pH_i during AP firing were compared with the dynamics of G_m in the AP-firing fibers treated with the PKC inhibitor, a close temporal correlation was observed (Fig. 3 E). Thus, although the majority of the reduction in G_m at the onset of AP firing was caused by PKC-mediated ClC-1 channel inhibition, the close temporal correlation between the dynamics of pH_i and G_m in PKC-inhibited EDL fibers indicates that acidification may have imposed a minor inhibitory effect on the ClC-1 channels.

The three groups of PKC isoforms that have thus far been discovered are distinguished by the cellular signals that convey their activation (Steinberg, 2008). Supposedly, the PKC inhibitors GF109203X and Gö6976 have the highest affinity for conventional PKC isoforms (Martiny-Baron et al., 1993), which require the presence of diacylglycerol as well as a rise in the free cytosolic Ca^{2+} for activation (Steinberg, 2008). To test whether the release of Ca^{2+} from the SR could be involved in activating the PKC-mediated ClC-1 channel inhibition, at the onset of AP firing a series of experiments was conducted in EDL fibers in which the Ca^{2+} release channels of the SR had been partially blocked by 25 μM dantrolene. In these fibers, the biphasic G_m dynamics that were usually observed in AP-firing EDL fibers were still observed

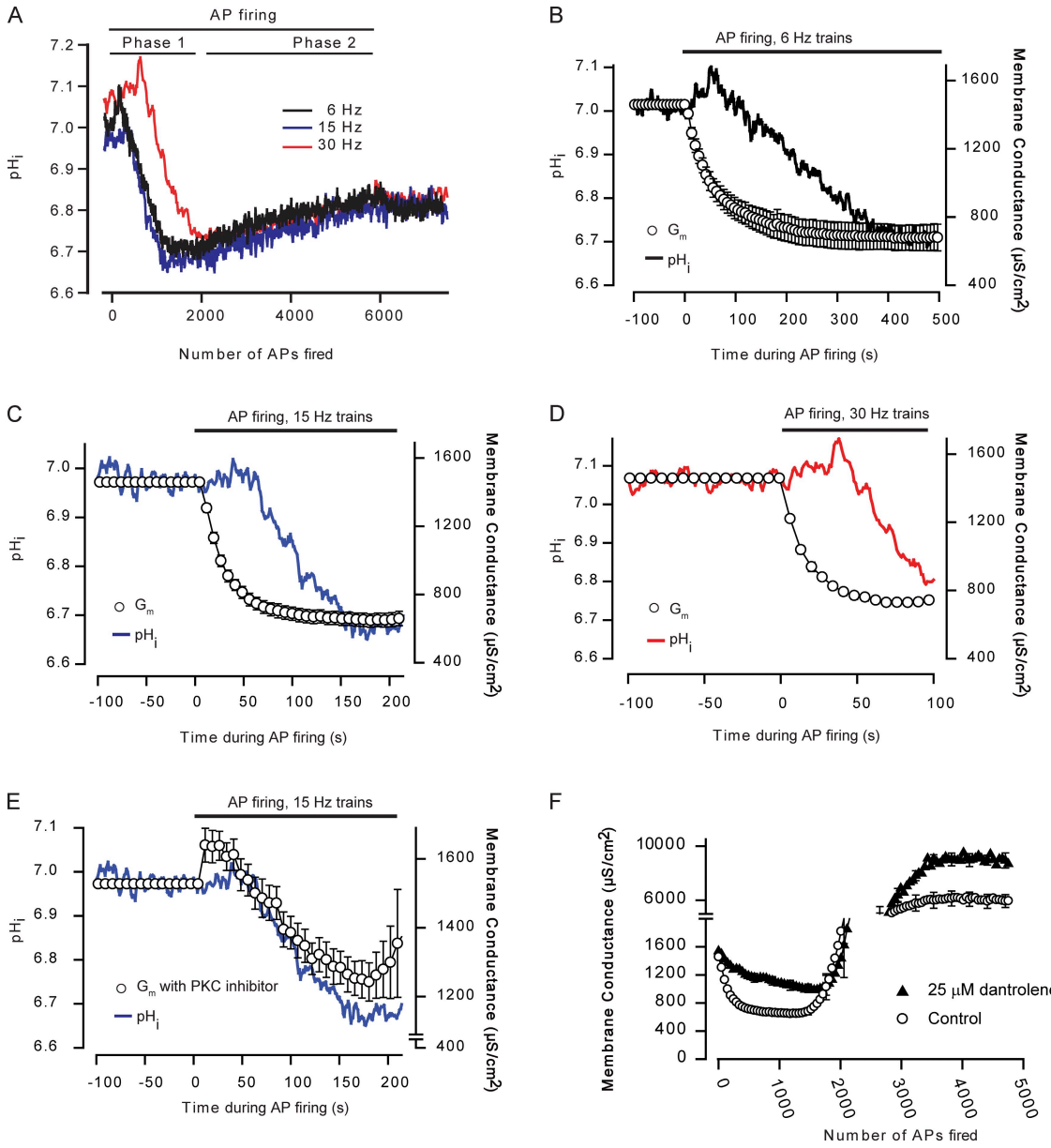

Figure 4. PKC-mediated ClC-1 channel inhibition at the onset of AP firing is not triggered by acidification. pH_i was recorded in whole EDL muscles exposed to field stimulation with 3.5-s trains every 7 s until 5,000 pulses had been delivered. The dynamics of pH_i and G_m were compared to evaluate their temporal relationship. (A) Recordings of pH_i during field stimulation of whole muscle with trains of 6, 15, or 30 Hz. Observations have been plotted against the total number of APs fired to illustrate the similar dependency of the dynamics of pH_i on the number of APs fired at the three frequencies. (B) The dynamics of pH_i and G_m in EDL fibers stimulated with 6-Hz trains. (C) The dynamics of pH_i and G_m during stimulation with 15-Hz trains. (D) The dynamics of pH_i and G_m when stimulated with 30-Hz trains. (E) The dynamics of pH_i in whole EDL muscles together with G_m from EDL fibers exposed to the PKC inhibitor. In B–E, pH_i and G_m have been plotted against the experimental duration. (F) G_m in EDL fibers firing APs in the presence of 25 µM dantrolene. Observations of G_m under control conditions have been included for comparison. Average data are presented as mean ± SEM.

(Fig. 4 F). However, with dantrolene, the reduction in G_m during Phase 1 was slower and less pronounced. Accordingly, the fitting of the observation to Eqs. 1 and 2 showed that τ_1 of Phase 1, which reflects how fast the PKC-mediated ClC-1 channel inhibition proceeded, was markedly increased with dantrolene, whereas A_1, which reflects the magnitude of the reduction of G_m, was not significantly affected (Table III). Hence, the primary effect of dantrolene was to slow the ClC-1 channel inhibition during Phase 1 and not to abolish it as occurred with the PKC inhibition.

Cellular mechanism underlying the activation of ClC-1 and K_{ATP} channels during Phase 2

An intriguing difference in the G_m dynamics between EDL and soleus fibers was the complete absence of

TABLE III

Parameters obtained by fitting blebbistatin observations of G_m at 15 to Eqs. 5 and 6

Muscle fiber type	Group	Myosin II inhibitor	A_1	τ_1	τ_1 (APs)	A_2	τ_2	τ_2 (APs)	β	β (APs)
			(μS/cm²)	*(s)*		*(μS/cm²)*	*(s)*		*(s)*	
EDL	15 Hz (n = 10) 25 μM dantrolene	BTS	−647 ± 38	—	565 ± 67	11,178 ± 2,101	—	2,566 ± 75	—	254 ± 24
EDL	15 Hz (n = 18) glucose free	BTS	−890 ± 26	—	170 ± 9	11,056 ± 1,143	—	2,127 ± 163	—	194 ± 33

Experimental observations of G_m in AP-firing EDL fibers with dantrolene or glucose-free conditions. A_2, τ_2, and β are as in Table II. All data are presented as means ± SEM.

Phase 2 in soleus fibers (Fig. 1). Our previous study (Pedersen et al., 2009) proposed that Phase 2 arose when the fibers reached a critical level of metabolic depression. This hypothesis is supported by the absence of Phase 2 in soleus fibers (Fig. 1 E) because these fibers have a higher content of mitochondria and a larger oxidative capacity than fast-twitch fibers (Jackman and Willis, 1996; Mogensen and Sahlin, 2005). The absence of elevated G_m with prolonged AP firing does not exclude that G_m can rise in these fibers because in experiments with carbonyl cyanide m-chlorophenylhydrazone, an uncoupler of mitochondria, the input conductance of resting soleus fibers increased immensely (not depicted). Still, to further evaluate a role of the metabolic state in the etiology of Phase 2, two more series of experiments were conducted in EDL fibers.

First, experiments were performed in which 6 min of rest were introduced after every 20th train of AP. The average observations from three such experiments are presented in Fig. 5. These observations show that by introducing resting periods of 6 min, G_m completely recovered after every set of 20 AP trains, and upon resumed AP firing, Phase 1 reappeared. Moreover, when compared with experiments without the intermittent resting periods, the appearance of Phase 2 became substantially delayed.

Second, a series of experiment was conducted with EDL fibers in glucose-free extracellular solution. Fig. 6 A

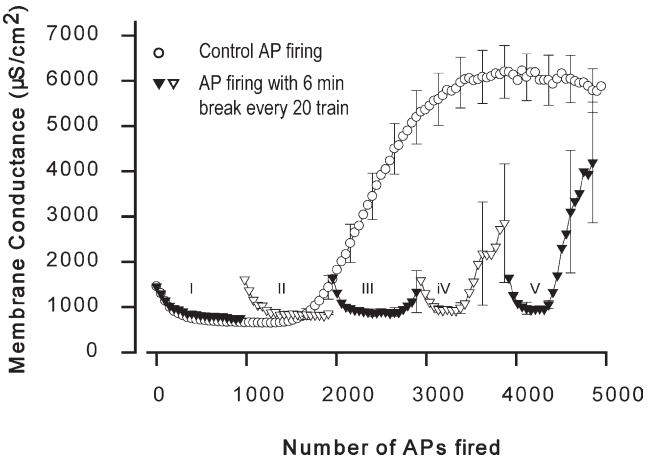

Figure 5. Phase 1 reappears and Phase 2 becomes delayed in EDL fibers when AP firing is interrupted by intermittent resting periods. Experiments were performed as described in Fig. 1, except that for every 20th train of AP, a resting period of 6 min was introduced. Five sets of 20 AP trains were fired in each fiber (I–V). Average G_m in three EDL fibers firing 15-Hz AP trains with intermittent resting periods after every 20th AP train. Recordings of G_m in similar fibers stimulated to fire APs without the intermittent resting periods have been included for comparison. Average data are presented as mean ± SEM.

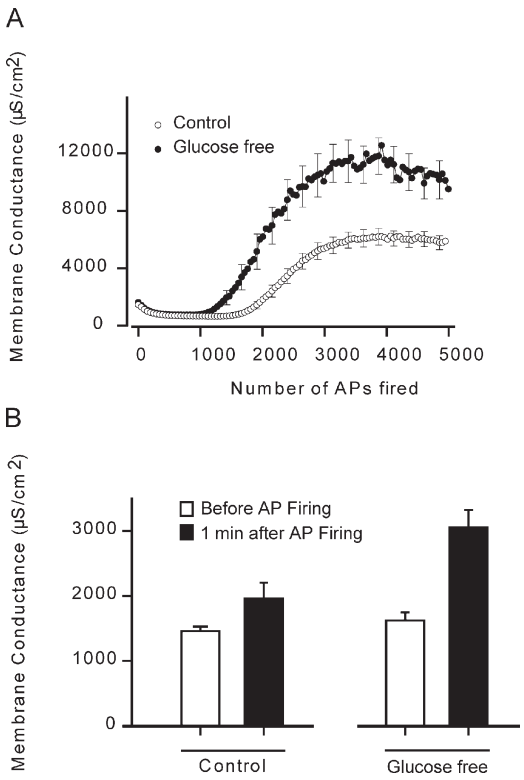

Figure 6. Glucose-free conditions accelerate the appearance of Phase 2 and enhance the magnitude of the rise in G_m during Phase 2. (A) G_m in 14 EDL fibers firing 15-Hz AP trains in the absence of extracellular glucose. Recordings of G_m under control conditions of 5 mM glucose have been included for comparison. (B) G_m before AP firing (G_mS, Table I) and G_m 1 min after firing 5,000 APs in the presence and absence of glucose. Average data are presented as mean ± SEM.

shows that at the onset of AP firing, G_m was reduced to a similar extent in the fibers in glucose-free and control conditions. Indeed, quantification showed that the magnitude of the reduction during Phase 1, A_1, was similar in the two situations, and that the time required for this reduction, τ_1, was also similar in the control fibers and in the fibers under glucose-free conditions (Table III). However, with prolonged AP firing, the fibers under glucose-free conditions entered Phase 2 before the control fibers, and G_m became substantially higher during Phase 2 in the fibers under glucose-free conditions than in the control fibers. Thus, quantification of Phase 2

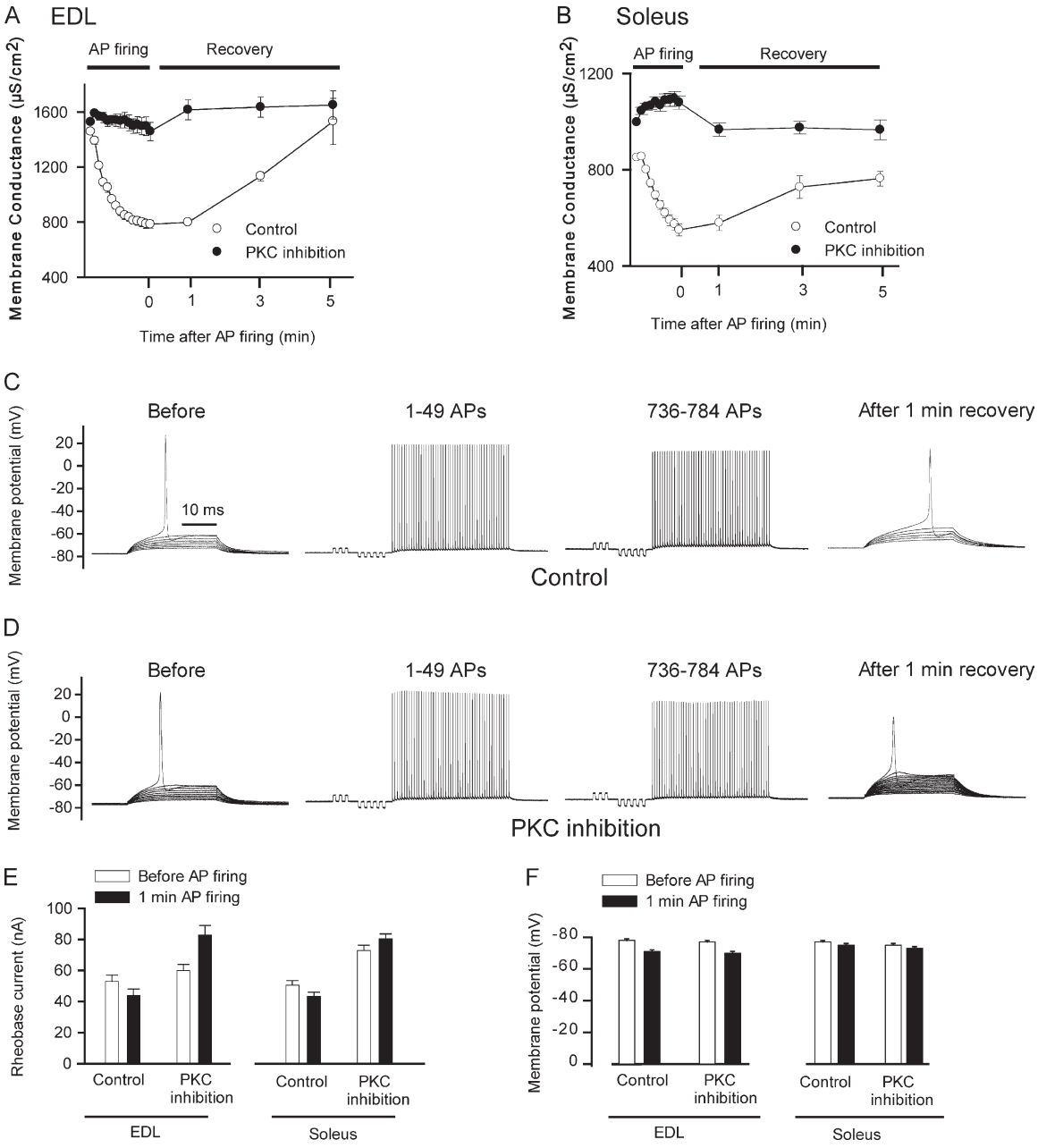

Figure 7. PKC-mediated ClC-1 inhibition at the onset of AP firing reduces the rheobase current in the fibers. (A and B) Under control conditions, the recovery of G_m after its initial reduction at the onset of AP firing lasted ~5 min in both EDL (A) and soleus fibers (B). Recordings of G_m in AP-firing fibers with the PKC inhibitor showed that G_m was not reduced at the onset of AP firing, and no change in G_m was observed during the recovery period. This was exploited to examine the role of PKC-mediated ClC-1 channel inhibition for the excitability of the fibers as evaluated by their rheobase current. (C) Membrane potential recordings in a control EDL fiber in which the rheobase current was measured before and 1 min after firing 784 APs. (D) Membrane potential recordings before AP firing and 1 min after firing 784 APs in an EDL fiber treated with PKC inhibitor (1 µM GF109203X). (E) Average rheobase currents in the two fiber types before and 1 min after AP firing in the presence or absence of the PKC inhibitor. (F) Average resting membrane potential before and 1 min after AP firing in the EDL and soleus fibers. Average data are presented as mean ± SEM.

with Eq. 2 showed that under glucose-free conditions, Phase 2 arose faster (τ_2 was 2,417 ± 127 APs and 2,127 ± 163 APs in control and in glucose-free conditions, respectively; $P < 0.05$) and reached a higher level than the in control fibers (A_2 was 5,426 ± 494 μS/cm^2 and 11,056 ± 1,143 μS/cm^2 in control and in glucose-free conditions, respectively; $P < 0.05$). Additionally, after 1 min of recovery from firing 4,998 APs, G_m only recovered partly in the absence of glucose, whereas a more complete recovery of G_m was observed in control conditions (Fig. 6 B).

Effect of G_m dynamics for the excitability of muscle

The physiological importance of the PKC-mediated ClC-1 channel inhibition for muscle excitability was next considered using two different experimental approaches.

First, the effect of PKC inhibition on muscle excitability was evaluated. Fig. 7 (A and B) demonstrates that if AP firing was ceased during the initial reduction in G_m, it lasted ~5 min for full recovery of G_m to be reached in both fiber types under control conditions. In contrast, neither EDL fibers nor soleus fibers showed any change in G_m during AP firing or during the subsequent recovery period if the fibers were pretreated with the PKC inhibitor. This slow recovery from the PKC inhibition of ClC-1 channels during Phase 1 in the control fibers was exploited to evaluate the role of ClC-1 channel inhibition for the fiber excitability by comparing the rheobase currents before and 1 min after AP firing in control fibers and in fibers with the PKC inhibitor. Fig. 7 C shows experimental recordings from a representative EDL fiber under control conditions, whereas Fig. 7 D shows recordings from a representative EDL fiber exposed to the PKC inhibitor. These recordings illustrate that when the rheobase current was assessed 1 min after AP firing, a marked reduction, indicative of increased excitability, was observed under control conditions. In contrast, in the fiber with the PKC inhibitor, the rheobase was substantially elevated after AP firing. Fig. 7 E shows the average rheobase currents before and after AP firing under control conditions and with PKC inhibition in both EDL and soleus fibers. In both fiber types, the rheobase was reduced after the short duration of AP firing under control conditions, whereas increased rheobase current was observed if PKC was inhibited. Note that similar changes in the resting membrane potential were observed after AP firing in the absence and presence of the PKC inhibitor in the two muscle fiber types (Fig. 7 F).

Second, the effect of pharmacological PKC activation for muscle fiber excitability was assessed in muscles at elevated extracellular K^+, which repeatedly has been used to experimentally compromise muscle excitability and contractile force (Nielsen et al., 2001; Pedersen et al., 2005). Fig. 8 shows representative recordings of M-waves (Fig. 8 A) and tetanic force (Fig. 8 B) from an intact soleus muscle when stimulated every 10 min with a 2-s long 60-Hz train. When extracellular K^+ was elevated from 4 to 10 mM, a pronounced decline in both M-waves (Fig. 8 A) and force (Fig. 8 B) took place. After 1 h at elevated extracellular K^+, PKC was activated by the addition of 5 μM of PKC activator, Pbdu, which resulted in a pronounced recovery of both the excitability (M-waves) and force. In four similar experiments, the

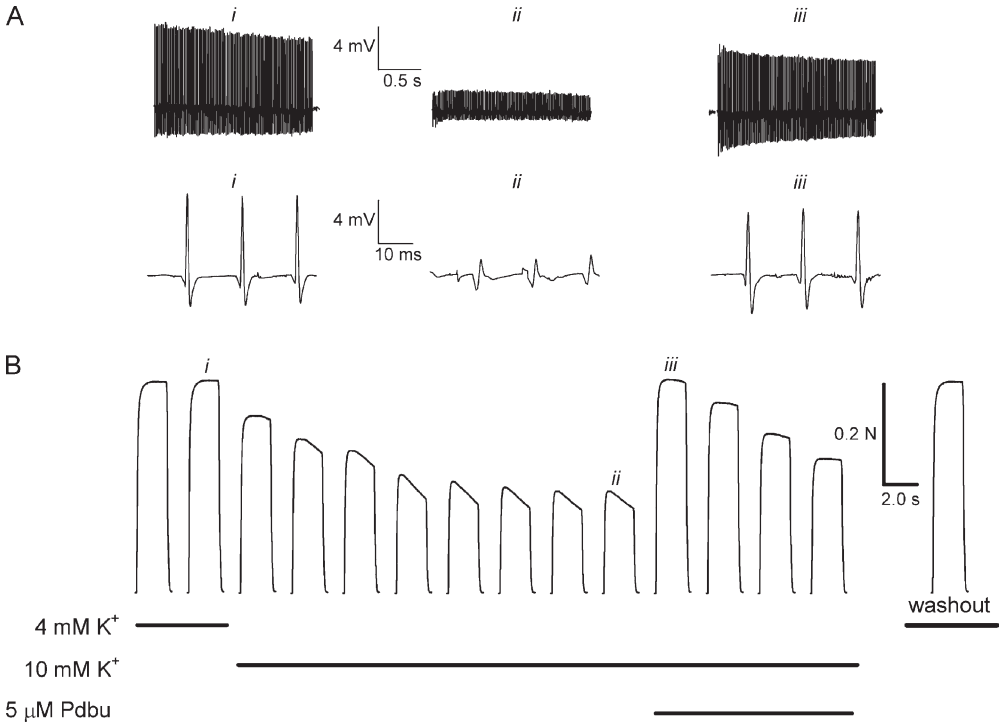

Figure 8. The PKC activator, Pbdu, recovers excitability and tetanic force in muscles depressed by elevated extracellular K^+. M-waves (A) and tetanic force (B) in response to field stimulation pulses (0.02 ms and 12 V at 60 Hz for 2 s) were recorded every 10 min in soleus muscles. Muscle excitability was assessed from M-waves. In the bottom of A, three successive M-waves from the M-wave trains in the top panel have been enlarged. Recordings were initially obtained at 4 mM K^+ and then at 10 mM K^+. After 1 h at 10 mM K^+, 5 μM Pbdu was added. After 40 min with Pbdu, 4 mM K^+ solution without the activator was reintroduced (washout).

addition of Pbdu to muscles at 10 mM K^+ caused the force to increase from 43 ± 5 to 76 ± 12% of the control force at 4 mM K^+. Similar results were obtained in two EDL muscles at 13 mM K^+ (not depicted).

DISCUSSION

This study demonstrates that in active, AP-firing skeletal muscle, the ion channels that determine G_m undergo substantial regulation in both fast- and slow-twitch muscle fibers. We show that in both fiber types, ClC-1 channels are rapidly inhibited at the onset of AP firing via a PKC-dependent pathway that becomes activated via AP-mediated SR Ca^{2+} release. Such ClC-1 channel inhibition increases the excitability of the fibers. We further show that the synchronous openings of ClC-1 and K_{ATP} channels with prolonged AP firing in EDL fast-twitch fibers do not occur in slow-twitch soleus fibers. We propose that a significant reduction in the metabolic state of the fibers may induce such ion channel activations in fast-twitch fibers and thereby support recent suggestions that ClC-1 channels are sensitive to the metabolic state of muscle fibers (Bennetts et al., 2005; Tseng et al., 2007; Zhang et al., 2008).

Increase in G_m after prolonged AP firing only occurs in fast-twitch fibers

In slow-twitch fibers, the onset of AP firing was associated with a reduction in G_m that, despite developing at a slower rate, was reminiscent of the ClC-1 channel inhibition that caused a reduction in G_m during Phase 1 in the fast-twitch fibers (Pedersen et al., 2009). Further support for this notion was provided by the observation that in both fiber types, the reduction in G_m at the onset of AP firing primarily reflected a pronounced reduction in G_{Cl}. Because the ClC-1 channel is generally considered to be the main Cl^- channel in muscle (Koch et al., 1992), and because G_{Cl} was reduced by as much as 70–80% at the onset of AP firing, reduced G_{Cl} must have also reflected ClC-1 channel inhibition in soleus fibers. Collectively, these observations show that the onset of muscle activity triggers a pronounced reduction in G_{Cl} that reflects underlying inhibition of ClC-1 channels in both fast- and slow-twitch muscle fibers.

In marked contrast to the similar G_m dynamics in the two fiber types during early stages of muscle activity, the two fiber types displayed strikingly different G_m dynamics after prolonged AP firing. Thus, in contrast to the development of a very large G_m after firing more than ~1,800 APs in EDL fibers, G_m in slow-twitch fibers remained low even after firing as many as 15,000 APs. If Phase 2 reflected a reduced metabolic state of the EDL fibers, as it will be argued below, it can be speculated that Phase 2 did not appear in slow-twitch fibers because these fibers have a larger oxidative capacity and hence would have a better preservation of their energetic state during repeated AP firing. Indeed, when the cellular metabolic state is evaluated after intensive contractions in muscles containing both fast- and slow-twitch fibers, the reduction in ATP and elevation in IMP are much more pronounced in the fast-twitch fibers as compared with slow-twitch fibers (Esbjörnsson-Liljedahl et al., 1999).

SR Ca^{2+} release triggers PKC-mediated ClC-1 channel inhibition at the onset of AP firing

Previous studies have demonstrated that ClC-1 channels can be inhibited by acidification and via intracellular pathways involving PKC (Hutter and Warner, 1967; Tricarico et al., 1991; Rosenbohm et al., 1999; Pedersen et al., 2004, 2005; Pierno et al., 2007; Dutka et al., 2008). Hence, to explore for a role of pH_i in ClC-1 channel inhibition at the onset of AP firing, the dynamics of pH_i in whole EDL muscle were measured during field stimulation and compared with the corresponding G_m dynamics. This showed that the majority of the ClC-1 channel inhibition occurred while the fibers were in an alkaline state, presumably caused by breakdown of creatine phosphate. Hence, the rapid ClC-1 channel inhibition at the onset of AP firing was not caused by acidification. In contrast, in both muscle fibers, the initial inhibition of ClC-1 channels during AP firing was largely abolished by PKC inhibition. The ClC-1 channel inhibition could also be partly prevented by blockage of SR Ca^{2+} channels with dantrolene. This indicates that Ca^{2+} release from SR during AP firing was important for activation of PKC. Such interactions between increased cytosolic Ca^{2+} and PKC for ClC-1 channel inhibition implicate the conventional PKC isoform in the inhibition, and this is supported by a recent study, which suggests that statin treatment of rats causes a chronic elevation in cytosolic Ca^{2+} that leads to PKC-mediated ClC-1 channel inhibition and hyperexcitability (Pierno et al., 2009). Because the reduction in G_m at the early stages of AP firing was well described by a single-exponential function in both muscles, it is likely that there was one rate-limiting step in the ClC-1 channel inhibition. Because dantrolene slowed down the process of ClC-1 inhibition at the onset of AP firing, it can be speculated that the rise in cytosolic Ca^{2+} represents this rate-limiting step in PKC-mediated ClC-1 inhibition in active muscle. Our observations demonstrate that the modulation of ClC-1 channels by statins (Pierno et al., 2009) that act via an elevated cytosolic Ca^{2+} reflects a physiological mechanism for inhibition of ClC-1 channels that occurs in active muscles. Thus, as summarized in Fig. 9, our findings demonstrate that during muscle activity, SR Ca^{2+} release triggered by AP firing activates PKC, which then inhibits the ClC-1 channels causing G_m to drop.

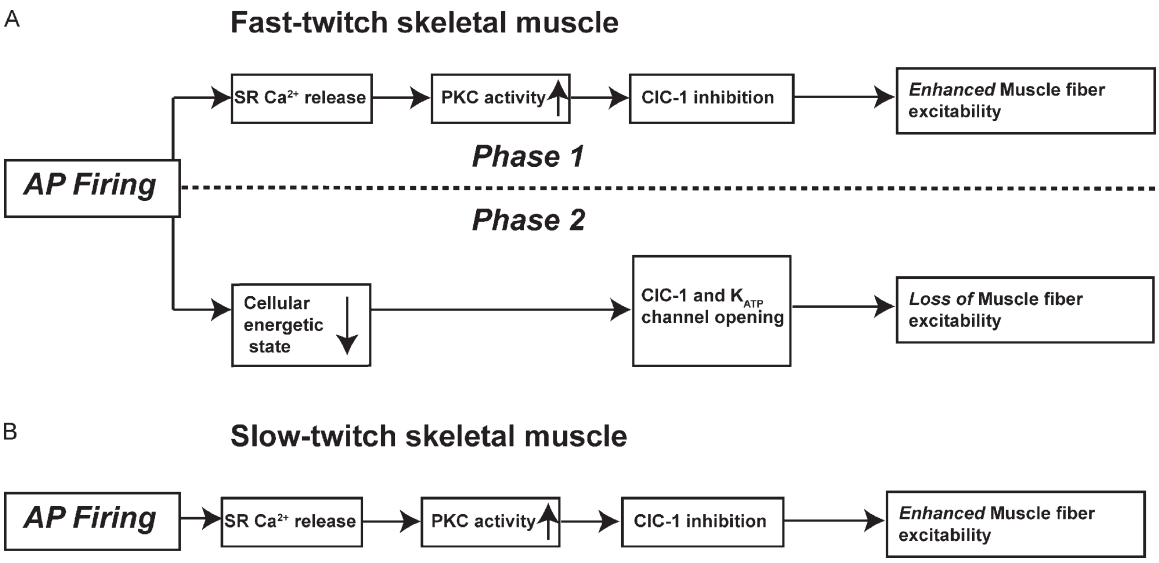

Figure 9. Diagram of observed G_m dynamics and underlying cellular mechanisms in AP-firing fast- (A) and slow-twitch (B) skeletal muscle fibers.

In both fiber types, full recovery from ClC-1 channel inhibition was observed after ~5 min. It is interesting that this was substantially longer than the time required for recovery of G_m after Phase 2 in the EDL fibers. This indicated that in fast-twitch fibers, the PKC-mediated inhibition of ClC-1 channels during Phase 1 disappeared once Phase 2 was initiated. The role of PKC for ClC-1 channel inhibition also implies that some proteins, possibly the ClC-1 channels, became phosphorylated. Thus, as it will be argued below, if Phase 2 reflected a substantial reduction in the metabolic state of the fibers, it is possible that dephosphorylation becomes predominant rather than PKC-mediated phosphorylation, when the ATP levels have declined substantially.

Further evidence of reduced metabolic state being the trigger for Phase 2

In our companion paper (Pedersen et al., 2009), it was demonstrated that the elevated G_m during Phase 2 in fast-twitch fibers reflected the opening of ClC-1 and K_{ATP} channels. In that study, it was hypothesized that the opening of these channels during Phase 2 reflected a substantial reduction in the metabolic state of the fibers. Three lines of evidence in favor of this hypothesis have been shown in the present study. First, the absence of Phase 2 in slow-twitch fibers supports the hypothesis that Phase 2 occurred in fast-twitch fibers when their metabolic state reached a critical level of depression. This support comes from the observations that slow-twitch fibers show less reduction in their cellular energetic state during prolonged contractile activity when compared with fast-twitch fibers (Esbjörnsson-Liljedahl et al., 1999). Second, a role of the metabolic state of the fibers for the induction of Phase 2 was implied by the early appearance and larger magnitude of Phase 2 in EDL fibers that were incubated under glucose-free conditions. These fibers were likely to have a moderately reduced metabolic state even before the AP firing and consequently would reach the level of metabolic depression required for the induction of Phase 2 faster than control fibers. Third, when resting periods of 6 min were introduced after every 20th train of AP, the appearance of Phase 2 was substantially postponed. This suggests that by introducing resting periods, the fibers were recovering their metabolic state in the resting periods sufficiently to delay the onset of Phase 2. Collectively, Phase 2 was accelerated if the muscles were exposed to either glucose-free conditions or prestimulated with field stimulation (Fig. S3 in Pedersen et al., 2009), it was delayed when AP trains had the lowest frequency (6 Hz) and when intermittent resting periods were introduced during the AP firing, and, finally, it was completely absent when explored in soleus fibers that have a larger oxidative capacity and show a better maintenance of the energetic state during activity (Esbjörnsson-Liljedahl et al., 1999). These findings can all be explained by the metabolic state of the fibers being a key determinant for the induction of Phase 2.

Functional significance of G_m dynamics for muscle function

Generally, the resting membrane conductance of muscle fibers and their excitability appear to be inversely related. Accordingly, the PKC-mediated ClC-1 channel inhibition at the onset of AP firing was associated with enhanced muscle fiber excitability, as indicated by a reduction in rheobase current after short-duration AP firing. Note that this effect could not be related to changes in the resting membrane potential because this was not affected by the PKC inhibitor before or after AP firing. Also, in experiments where the muscle excitability

was initially depressed by exposing whole muscles to elevated extracellular K^+, PKC activation with a phorbol ester markedly recovered the excitability. Using a similar experimental approach of elevated extracellular K^+, we have previously shown that ClC-1 channel inhibition either via acidification or directly by the addition of 9-AC can recover muscle excitability in both fast- and slow-twitch muscles (Nielsen et al., 2001; Pedersen et al., 2004, 2005). Thus, the addition of the phorbol ester, which is known to reduce the resting G_{Cl} in rat muscle (Tricarico et al., 1991), is likely to have mediated the recovery of excitability and force in K^+ depressed via inhibition of ClC-1 channels, although other mechanisms may contribute.

Collectively, these observations suggest a scenario in which at the onset of muscle activity, AP-mediated SR Ca^{2+} release leads to an increased PKC activity, which in turn inhibits the ClC-1 channels and thereby enhances the excitability of the working muscle (Fig. 9). Conversely, the openings of ClC-1 and K_{ATP} channels during Phase 2, which was exclusive for fast-twitch fibers, resulted in increased G_m and dropout of APs (Fig. 9). It can be speculated that such a mechanism may contribute to the larger fatigability of fast-twitch fibers, and could serve as a protective mechanism that, by hindering prolonged muscle activation, limits metabolic depletion and excessive fiber damage during exercise. This notion is supported by observations of severe muscle damage in K_{ATP} channel knockout mice after treadmill running (Thabet et al., 2005; Cifelli et al., 2007).

Conclusion

In combination with our previous study (Pedersen et al., 2009), our findings demonstrate for the first time that acute regulation of G_m is a general phenomenon in active muscle. Our studies also show that this G_m regulation results from changes in the functions of ClC-1 and K_{ATP} channels and, thereby, reveal new physiological aspects on ClC-1 and K_{ATP} channels in skeletal muscles. In so doing, our observations complement several previous studies that have focused on specific pathways for ion channel regulation. Our approach allows for the determination of whether and when G_m is regulated in AP-firing fibers and which cellular signaling pathways that are involved. Because the observed changes in G_m had significant effects on muscle fiber excitability, our observations indicate that the excitability of skeletal muscles is far more dynamically regulated during muscle activity than previously expected.

Furthermore, the regulation of G_m differs significantly between fast- and slow-twitch fibers, with fast-twitch fibers being much more prone to a regulated reduction in excitability via massively elevated G_m. This fits with slow-twitch fibers often being involved in low intensity but prolonged contractile activity in the intact organism, whereas fast-twitch fibers usually are involved in intensive contractions of short duration. As such, the observed regulation of G_m may contribute to these well-established differences in the phenotypes of fast- and slow-twitch fibers.

We thank T.L. Andersen, V. Uhre, and M. Stürup-Johansen for technical assistance. Dr. J.A. Flatman is acknowledged for helpful discussions of the experiments and for assistance in writing the manuscript. Professor Christian Ålkjær is acknowledged for technical assistance in experiments performed to determine pH_i.

This work was supported by The Danish Research Medical Council (to T.H. Pedersen and O.B. Nielsen) and the Faculty of Health Science, University of Århus (to T.H. Pedersen and F. de Paoli).

Christopher Miller served as editor.

Submitted: 6 July 2009
Accepted: 11 September 2009

REFERENCES

Bennetts, B., G.Y. Rychkov, H.L. Ng, C.J. Morton, D. Stapleton, M.W. Parker, and B.A. Cromer. 2005. Cytoplasmic ATP-sensing domains regulate gating of skeletal muscle ClC-1 chloride channels. *J. Biol. Chem.* 280:32452–32458. doi:10.1074/jbc.M502890200

Cheung, A., J.A. Dantzig, S. Hollingworth, S.M. Baylor, Y.E. Goldman, T.J. Mitchison, and A.F. Straight. 2002. A small-molecule inhibitor of skeletal muscle myosin II. *Nat. Cell Biol.* 4:83–88. doi:10.1038/ncb734

Cifelli, C., F. Bourassa, L. Gariépy, K. Banas, M. Benkhalti, and J.M. Renaud. 2007. K_{ATP} channel deficiency in mouse flexor digitorum brevis causes fibre damage and impairs Ca^{2+} release and force development during fatigue in vitro. *J. Physiol.* 582:843–857. doi:10.1113/jphysiol.2007.130955

de Paoli, F.V., K. Overgaard, T.H. Pedersen, and O.B. Nielsen. 2007. Additive protective effects of the addition of lactic acid and adrenaline on excitability and force in isolated rat skeletal muscle depressed by elevated extracellular K^+. *J. Physiol.* 581:829–839. doi:10.1113/jphysiol.2007.129049

Dutka, T.L., R.M. Murphy, D.G. Stephenson, and G.D. Lamb. 2008. Chloride conductance in the transverse tubular system of rat skeletal muscle fibres: importance in excitation-contraction coupling and fatigue. *J. Physiol.* 586:875–887. doi:10.1113/jphysiol.2007.144667

Edström, L., E. Hultman, K. Sahlin, and H. Sjöholm. 1982. The contents of high-energy phosphates in different fibre types in skeletal muscles from rat, guinea-pig and man. *J. Physiol.* 332:47–58.

Esbjörnsson-Liljedahl, M., C.J. Sundberg, B. Norman, and E. Jansson. 1999. Metabolic response in type I and type II muscle fibers during a 30-s cycle sprint in men and women. *J. Appl. Physiol.* 87:1326–1332.

Hutter, O.F., and A.E. Warner. 1967. The pH sensitivity of the chloride conductance of frog skeletal muscle. *J. Physiol.* 189:403–425.

Jackman, M.R., and W.T. Willis. 1996. Characteristics of mitochondria isolated from type I and type IIb skeletal muscle. *Am. J. Physiol.* 270:C673–C678.

Koch, M.C., K. Steinmeyer, C. Lorenz, K. Ricker, F. Wolf, M. Otto, B. Zoll, F. Lehmann-Horn, K.H. Grzeschik, and T.J. Jentsch. 1992. The skeletal muscle chloride channel in dominant and recessive human myotonia. *Science.* 257:797–800. doi:10.1126/science.1379744

Limouze, J., A.F. Straight, T. Mitchison, and J.R. Sellers. 2004. Specificity of blebbistatin, an inhibitor of myosin II. *J. Muscle Res. Cell Motil.* 25:337–341. doi:10.1007/s10974-004-6060-7

Lueck, J.D., A. Mankodi, M.S. Swanson, C.A. Thornton, and R.T. Dirksen. 2007. Muscle chloride channel dysfunction in two mouse models of myotonic dystrophy. *J. Gen. Physiol.* 129:79–94. doi:10.1085/jgp.200609635

Macdonald, W.A., T.H. Pedersen, T. Clausen, and O.B. Nielsen. 2005. N-Benzyl-p-toluene sulphonamide allows the recording of trains of intracellular action potentials from nerve-stimulated intact fast-twitch skeletal muscle of the rat. *Exp. Physiol.* 90:815–825. doi:10.1113/expphysiol.2005.031435

Martiny-Baron, G., M.G. Kazanietz, H. Mischak, P.M. Blumberg, G. Kochs, H. Hug, D. Marmé, and C. Schächtele. 1993. Selective inhibition of protein kinase C isozymes by the indolocarbazole Gö 6976. *J. Biol. Chem.* 268:9194–9197.

Mogensen, M., and K. Sahlin. 2005. Mitochondrial efficiency in rat skeletal muscle: influence of respiration rate, substrate and muscle type. *Acta Physiol. Scand.* 185:229–236. doi:10.1111/j.1365-201X.2005.01488.x

Nielsen, O.B., F. de Paoli, and K. Overgaard. 2001. Protective effects of lactic acid on force production in rat skeletal muscle. *J. Physiol.* 536:161–166. doi:10.1111/j.1469-7793.2001.t01-1-00161.x

Pedersen, T.H., O.B. Nielsen, G.D. Lamb, and D.G. Stephenson. 2004. Intracellular acidosis enhances the excitability of working muscle. *Science.* 305:1144–1147. doi:10.1126/science.1101141

Pedersen, T.H., F. de Paoli, and O.B. Nielsen. 2005. Increased excitability of acidified skeletal muscle: role of chloride conductance. *J. Gen. Physiol.* 125:237–246. doi:10.1085/jgp.200409173

Pedersen, T.H., F.V. de Paoli, J.A. Flatman, and O.B. Nielsen. 2009. Regulation of ClC-1 and KATP channels in action potential–firing fast-twitch muscle fibers. *J. Gen. Physiol.* 134:309–322.

Pierno, S., J.F. Desaphy, A. Liantonio, A. De Luca, A. Zarrilli, L. Mastrofrancesco, G. Procino, G. Valenti, and D. Conte Camerino. 2007. Disuse of rat muscle in vivo reduces protein kinase C activity controlling the sarcolemma chloride conductance. *J. Physiol.* 584:983–995. doi:10.1113/jphysiol.2007.141358

Pierno, S., G.M. Camerino, V. Cippone, J.F. Rolland, J.F. Desaphy, A. De Luca, A. Liantonio, G. Bianco, J.D. Kunic, A.L. George Jr., and D. Conte Camerino. 2009. Statins and fenofibrate affect skeletal muscle chloride conductance in rats by differently impairing ClC-1 channel regulation and expression. *Br. J. Pharmacol.* 156:1206–1215. doi:10.1111/j.1476-5381.2008.00079.x

Rosenbohm, A., R. Rüdel, and C. Fahlke. 1999. Regulation of the human skeletal muscle chloride channel hClC-1 by protein kinase C. *J. Physiol.* 514:677–685. doi:10.1111/j.1469-7793.1999.677ad.x

Steinberg, S.F. 2008. Structural basis of protein kinase C isoform function. *Physiol. Rev.* 88:1341–1378. doi:10.1152/physrev.00034.2007

Straight, A.F., A. Cheung, J. Limouze, I. Chen, N.J. Westwood, J.R. Sellers, and T.J. Mitchison. 2003. Dissecting temporal and spatial control of cytokinesis with a myosin II Inhibitor. *Science.* 299:1743–1747. doi:10.1126/science.1081412

Thabet, M., T. Miki, S. Seino, and J.M. Renaud. 2005. Treadmill running causes significant fiber damage in skeletal muscle of K_{ATP} channel-deficient mice. *Physiol. Genomics.* 22:204–212. doi:10.1152/physiolgenomics.00064.2005

Thomas, J.A., R.N. Buchsbaum, A. Zimniak, and E. Racker. 1979. Intracellular pH measurements in Ehrlich ascites tumor cells utilizing spectroscopic probes generated in situ. *Biochemistry.* 18:2210–2218. doi:10.1021/bi00578a012

Toullec, D., P. Pianetti, H. Coste, P. Bellevergue, T. Grand-Perret, M. Ajakane, V. Baudet, P. Boissin, E. Boursier, F. Loriolle, et al. 1991. The bisindolylmaleimide GF 109203X is a potent and selective inhibitor of protein kinase C. *J. Biol. Chem.* 266:15771–15781.

Tricarico, D., D. Conte Camerino, S. Govoni, and S.H. Bryant. 1991. Modulation of rat skeletal muscle chloride channels by activators and inhibitors of protein kinase C. *Pflugers Arch.* 418:500–503. doi:10.1007/BF00497778

Tseng, P.Y., B. Bennetts, and T.Y. Chen. 2007. Cytoplasmic ATP inhibition of CLC-1 is enhanced by low pH. *J. Gen. Physiol.* 130:217–221. doi:10.1085/jgp.200709817

Zhang, S.J., D.C. Andersson, M.E. Sandström, H. Westerblad, and A. Katz. 2006. Cross bridges account for only 20% of total ATP consumption during submaximal isometric contraction in mouse fast-twitch skeletal muscle. *Am. J. Physiol. Cell Physiol.* 291:C147–C154. doi:10.1152/ajpcell.00578.2005

Zhang, X.D., P.Y. Tseng, and T.Y. Chen. 2008. ATP inhibition of CLC-1 is controlled by oxidation and reduction. *J. Gen. Physiol.* 132:421–428. doi:10.1085/jgp.200810023